ELSEVIER

Earth and Planetary Science Letters 206 (2003) 617–625

EPSL

www.elsevier.com/locate/epsl

Substitution mechanism of Al ions in $MgSiO_3$ perovskite under high pressure conditions from first-principles calculations

Tomoyuki Yamamoto [a,*], David A. Yuen [b], Toshikazu Ebisuzaki [a]

[a] *Computational Science Division, RIKEN, 2-1 Hirosawa, Wako-shi, Saitama 351-0198, Japan*
[b] *Department of Geology and Geophysics and Minnesota Supercomputing Institute, University of Minnesota, Minneapolis, MN 55455-0219, USA*

Received 22 July 2002; received in revised form 8 November 2002; accepted 13 November 2002

Abstract

Large-scale first-principles density functional theory (DFT) calculations have been carried out to investigate how Al^{3+} can be incorporated into $MgSiO_3$ perovskite under high pressure and to study the resultant change in the compressional mechanism of $MgSiO_3$ perovskite. We examined two types of $MgSiO_3$ models with 6.25 mol% Al_2O_3: charge-coupled substitution and oxygen-vacancy mechanisms. Five pressure points from 0 to 100 GPa have been considered. At each pressure point, we have calculated five models of the oxygen vacancy and five models of the charge-coupled mechanisms. We also change the internal positions of the substituted Al in the calculated cells, which have 80 atoms. Our free energy calculations show Al^{3+} replaces the nearest-neighbor cation pairs (Mg^{2+} and Si^{4+}) at all pressures investigated. The calculated bulk modulus of the most energetically favorable model is 3.4% lower than that of the Al-free $MgSiO_3$ perovskite. These results may have important implications for discriminating between thermal and compositional effects of 1-D Earth models and the possible influence of aluminum perovskite.

Keywords: aluminous perovskite; first-principles calculations; substitution mechanism; bulk modulus

1. Introduction

The structural and elastic properties of materials under high pressure and temperature conditions have been extensively studied both experimentally [1] and theoretically [2]. These kinds of studies have provided the geophysical community with fundamental knowledge, such as the phonon spectra, of many material properties under physical conditions characteristic of the deep mantle, and improve the modeling efforts of mantle convection with realistic parameters for the equation of state. Most geoscientists believe that the dominant mineral phases of the Earth's lower mantle are essentially $MgSiO_3$ with the perovskite structure and magnesiowüstite [3]. Therefore, the high-

* Corresponding author. Present address: Fukui Institute for Fundamental Chemistry, Kyoto University, 34-4 Takano-nishibirakicho, Sakyo-ku, Kyoto-shi, Kyoto 606-8103, Japan. Tel.: +81-75-753-5454; Fax: +81-75-753-5447.
E-mail address: tyama@cms.mtl.Kyoto-u.ac.jp (T. Yamamoto).

0012-821X/02/$ – see front matter
doi:10.1016/S0012-821X(02)01099-3

pressure behavior of $MgSiO_3$ perovskite pertains to a wide range of geophysical problems, and has been widely studied both experimentally [4,5] and theoretically [6–10].

Recently, it was reported that small amounts of Al ions incorporated into $MgSiO_3$ perovskite can drastically change the bulk properties [11,12]. After ferric and ferrous iron, Al^{3+} is the most abundant cation in solid solution in this phase. About 4–5 mol% Al_2O_3 is present in all proposed lower mantle compositions, and it is believed that all Al ions are incorporated into $MgSiO_3$ perovskite under lower mantle pressure and temperature conditions [13]. When $MgSiO_3$ perovskite contains 5–10 wt% Al_2O_3, high pressure experiments suggest the bulk modulus becomes significantly lower, −10% or more, than that of pure $MgSiO_3$ perovskite [11,12].

Two mechanisms of substitution have been proposed for Al ions incorporation into $MgSiO_3$ perovskite [14]. For a charge-coupled mechanism (CCM), two Al^{3+} ions replace pairs of Mg^{2+} and Si^{4+} ions in nearest-neighbor sites. No oxygen vacancies are required for charge balance. The second one is an oxygen-vacancy mechanism (OVM), $2Al^{3+} \rightarrow 2Si^{4+}+O^{2-}$. In this case, two Al^{3+} ions replace two Si^{4+} ions and an oxygen ion. It is necessary to remove an oxygen ion to balance charge. Recent Al XAFS study [15] suggested CCM should be the most possible mechanism, and more clearly Stebbins et al. reported the NMR results [16], in which only CCM was detected for the substitution mechanism of Al^{3+} into $MgSiO_3$ perovskite. The empirical molecular mechanics simulations [14] also favor CCM over OVM at pressures characteristic of the lower mantle. Recently, Brodholt reported the first-principles DFT (density functional theory) [17] results on aluminous perovskite [18], in which OVM should be favored at shallower parts of the lower mantle up to about 30 GPa. The small sizes of cells, i.e. $(Mg_3Al)(Si_3Al)O_{12}$ perovskite and $Mg_2Al_2O_5$ brownmillerite, used in Brodholt's calculations can only represent highly ordered Al-incorporated structures. High concentrations of Al_2O_3, 25 mol%, are considered for CCM in $(Mg_3Al)(Si_3Al)O_{12}$ perovskite, and no Si was taken into account for OVM in $Mg_2Al_2O_5$ brownmillerite.

In order to investigate how Al^{3+} is incorporated into the $MgSiO_3$ perovskite structure and how the compressional mechanism of Al-incorporated $MgSiO_3$ perovskite changes, we carried out first-principles DFT calculations with large supercells consisting of 80 atoms and corresponding to 6.25 mol% Al_2O_3 incorporation. We find that the CCM is more favorable than the OVM at all pressures up to 100 GPa. Although our present calculations cannot explain the experimental reduction of bulk modulus (−10% [11]) due to Al^{3+} incorporation, both of these mechanisms reveal the same tendencies, as found in the experiments [11].

2. Calculational procedures

Our calculational methods call for the use of DFT [17] and the plane-wave pseudopotential method [19]. The effective exchange-correlation functional GGA-PBE [20] and Vanderbilt-type ultrasoft pseudopotentials [21] were used with a plane-wave cutoff of 380 eV. A Monkhorst–Pack *k*-point grid [22] with a spatial resolution of 0.1 $Å^{-1}$ was used for all structures. All the calculations were performed using the academic version of CASTEP (CAmbridge Serial Total Energy Package) code [17] at 0 K. In these calculations, three-dimensional periodic boundary conditions are taken into account.

At first, a $2\times2\times1$ super-cell with *Pbnm* symmetry, which contains 80 atoms, was used for Al-free $MgSiO_3$, in which all the atomic positions and cell parameters were allowed to relax. This computation allows direct comparison of the bulk properties of Al-rich and Al-free perovskite. We optimized the cell parameters and the enthalpies, i.e. Gibbs' free energies at 0 K ($E+PV$), at 0, 25, 50, 75 and 100 GPa. Because there are several possible atomic configurations in the cells for Al-incorporation through OVM and CCM, we calculated five different OVMs and five different CCMs changing their atomic configurations in order to determine which atomic configuration is most favorable. In OVM1, a nearest-neighbor pair of two Si^{4+} is replaced by two Al^{3+} ions and O^{2-} between these two Si^{4+} is removed to keep charge

Table 1
Initial internal atomic positions of substituted ions for Al-incorporated $MgSiO_3$ perovskite

	$Si^{4+} \rightarrow Al^{3+}$	$Si^{4+} \rightarrow Al^{3+}$	Oxygen vacancy
OVM1	(0.25, 0.5, 0.5)	(0.5, 0.25, 0.5)	(0.4, 0.4, 0.45)
OVM2	(0.25, 0.5, 0.5)	(0.5, 0.25, 0.5)	(0.65, 0.35, 0.55)
OVM3	(0.25, 0.5, 0.5)	(0.5, 0.25, 0.5)	(0.6, 0.1, 0.55)
OVM4	(0, 0.75, 0.5)	(0.5, 0.25, 0.5)	(0.6, 0.1, 0.55)
OVM5	(0, 0.75, 0.5)	(0.5, 0.25, 0.5)	(0.45, 0.77, 0.75)
	$Si^{4+} \rightarrow Al^{3+}$	$Mg^{2+} \rightarrow Al^{3+}$	
CCM1	(0.5, 0.25, 0.5)	(0.51, 0.47, 0.75)	
CCM2	(0.5, 0.25, 0.5)	(0.74, 0.22, 0.75)	
CCM3	(0.5, 0.25, 0.5)	(0.49, 0.53, 0.25)	
CCM4	(0.5, 0.25, 0.5)	(0.24, 0.72, 0.75)	
CCM5	(0.5, 0.25, 0.5)	(0.01, 0.97, 0.75)	

balance. In OVM2 and OVM3 two Al^{3+} are substituted as OVM1, although an oxygen vacancy is created at positions (0.65, 0.35, 0.55) and (0.6, 0.1, 0.55), respectively, which are attached to one of the Al^{3+} ions. In OVM4, two distant Si^{4+} ions are replaced by two Al^{3+} ions and an oxygen vacancy is created at (0.6, 0.1, 0.55), which is attached to one of the incorporated Al^{3+}. In OVM5, two Al^{3+} ions are substituted as in OVM4, although an oxygen vacancy is created at (0.45, 0.77, 0.75), which does not attach to any Al^{3+} ions. In CCM1, a nearest-neighbor pair of Mg^{2+} and Si^{4+} ions is replaced by two Al^{3+} ions, whereas distant pairs of Mg^{2+} and Si^{4+} are replaced by two Al^{3+} ions in CCM2–CCM5. Distances between two substituted Al^{3+} ions for CCM1, CCM2, CCM3, CCM4 and CCM5 are 2.79, 2.91, 3.24, 5.54 and 5.72 Å, respectively. Table 1 lists all the internal atomic positions for the substituted ions in the calculated super-cells. First-principles DFT calculations for these OVMs and CCMs were done in the same manner as for pure $MgSiO_3$ perovskite.

To compare the enthalpy difference between those with and without Al ions, we also performed the first-principles DFT calculations for Al_2O_3 and MgO, in which the unit cells of Al_2O_3 and MgO with corundum- and NaCl-type structures were considered, respectively.

All the calculations were carried out using the FUJITSU VPP700E vector parallel supercomputer installed in RIKEN. Although the CASTEP code here employed has been highly optimized for this vector computer, it still takes about 20 h of wallclock time with eight processors to derive the optimal crystallographic structure of a single model. Here we optimized 11 models with different crystallographic structures at five pressure points, which required about 1000 h wallclock time in total with eight processors in use on this vector parallel supercomputer.

3. Results

Table 2 summarizes the calculated cell parameters, volumes and enthalpies of Al-free $MgSiO_3$ perovskite as a function of pressure. In this table, the cell parameters and volumes are transferred to the ones for unit cells to compare directly with experiments and other calculations, whereas the enthalpies are for the calculated super-cells. In order to obtain an isothermal bulk modulus, calculated volumes are fitted to the third-order Birch–Murnaghan equation of state with $dB/dP = 4$, where B and P are the isothermal bulk modulus and the pressure, respectively. We have found good agreement of the cell parameters and volume for Al-free $MgSiO_3$ perovskite between experiment [4] and calculation at zero pressure, in which differences in cell parameters and volumes at 0 GPa between these two are less than 0.6% and 0.4%, respectively, whereas the calculated bulk modulus (236 GPa) was −9.6% too low, as is typical with the GGA calculations.

To determine which Al-incorporated model is the most favorable of the five OVMs and five

Table 2
Calculated unit cell parameters, a, b and c, volumes, V, and enthalpies, H[a], as a function of pressure, P, for Al-free $MgSiO_3$ perovskite

P (GPa)	a (Å)	b (Å)	c (Å)	V (Å^3)	H (eV)[a]
0	4.803	4.929	6.900	163.35	−38529.58
25	4.655	4.802	6.673	149.18	−38432.42
50	4.540	4.702	6.549	139.79	−38342.35
75	4.472	4.641	6.399	132.83	−38257.31
100	4.381	4.570	6.319	126.52	−38176.38

[a] Values for calculated super-cells.

Table 3
Calculated enthalpies, H, of Al-incorporated models, CCM and OVM, as a function of pressure, P

P (GPa)	H (eV)				
	OVM1	OVM2	OVM3	OVM4	OVM5
0	−37988.83	−37988.83	−37988.64	−37988.89	−37988.78
25	−37890.70	−37890.44	−37890.18	−37890.49	−37890.11
50	−37800.09	−37799.69	−37799.48	−37799.72	−37799.13
75	−37714.77	−37714.23	−37714.02	−37714.25	−37713.56
100	−37633.63	−37632.96	−37632.77	−37633.02	−37632.20
	CCM1	CCM2	CCM3	CCM4	CCM5
0	−37559.04	−37558.93	−37558.93	−37558.86	−37558.96
25	−37461.75	−37461.73	−37461.69	−37461.59	−37461.68
50	−37371.70	−37371.67	−37371.57	−37371.35	−37371.59
75	−37286.76	−37286.70	−37286.65	−37286.51	−37286.56
100	−37205.88	−37205.82	−37205.75	−37205.60	−37205.65

CCMs, we have compared the enthalpies of these calculated OVMs and CCMs as a function of pressure (Table 3). Enthalpy differences relative to CCM1 or OVM1 are shown in Fig. 1A,B. Model CCM1 is most favorable at all pressures up to 100 GPa (Fig. 1A). The OVM4 is most stable at 0 GPa, but the OVM1 is most favorable at higher pressures between 25 and 100 GPa within the OVM configuration (Fig. 1B). The enthalpy differences between OVM1 and other OVMs increase incrementally with pressure as shown in Fig. 1B, while those between CCM1 and the other CCMs do not change much.

Geometrical structures of the calculated super-cells optimized at 25 GPa for Al-free and two favorable Al-incorporated models, CCM1 and OVM1, are shown, respectively, in Fig. 2A–C. From the results of enthalpy calculations, in

Table 4
Calculated volumes, V, of Al-incorporated models, CCM and OVM, as a function of pressure, P

P (GPa)	V (Å^3)				
	OVM1	OVM2	OVM3	OVM4	OVM5
0	165.35	165.80	165.87	165.84	165.38
25	150.37	150.79	150.80	150.79	151.19
50	140.26	140.61	140.60	140.89	140.97
75	132.95	132.77	132.77	133.04	133.18
100	126.67	126.84	126.84	126.76	126.79
B (GPa)	220(−6.8%)	218(−7.6%)	217(−8.1%)	218(−7.6%)	215(−8.9%)
	CCM1	CCM2	CCM3	CCM4	CCM5
0	163.69	163.45	163.53	163.59	163.60
25	149.49	149.39	149.45	149.49	149.55
50	139.66	129.43	139.95	139.72	139.69
75	132.19	132.28	132.29	132.33	132.39
100	126.17	126.11	126.35	126.42	126.48
B (GPa)	228(−3.4%)	230(−2.5%)	232(−1.7%)	230(−2.5%)	232(−1.7%)

Volumes are 1/4 of calculated super-cells for the direct comparison with experiments and calculations for Al-free $MgSiO_3$ perovskite. Bulk moduli, B, are obtained with third-order Birch–Murnaghan fitting. Differences in bulk moduli relative to the calculated one for Al-free perovskite are expressed as percent in parentheses.

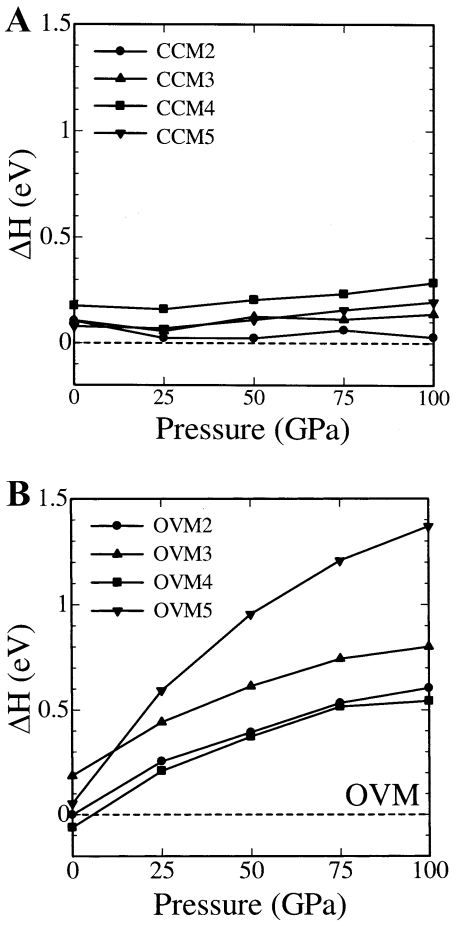

Fig. 1. Enthalpies of Al-incorporated models for (A) CCM and (B) OVM as functions of pressures relative to (A) CCM1 and (B) OVM1, respectively.

both favorable substitutions, we find that the OVM1 and CCM1, nearest-neighbor pairs of Si^{4+} ions or of Mg^{2+} and Si^{4+}, are replaced by two Al^{3+} ions at all pressures beyond 25 GPa.

Volumes (Table 4) of the most favorable models at zero pressure, i.e. CCM1 and OVM4, are +0.2% and +1.5% larger than that of pure $MgSiO_3$, respectively, both of which suggest the same tendencies as the experimental results (+0.5%) [11]. The calculated bulk moduli of all Al^{3+}-incorporated models (bottom line in Table 4) are −1.7% to −8.9% lower than that of Al-free $MgSiO_3$ perovskite. The calculated bulk moduli of OVMs are much lower than CCMs (Table 3). These calculated reductions of the bulk moduli due to Al substitutions show the same tendencies as the experiments, but our present calculations cannot entirely explain the experiments, which provide a larger reduction (−10%) [11].

Calculated equilibrium cell parameters at zero pressure and bulk modulus of MgO are 4.270 Å and 156 GPa, respectively, which reproduce the experimental cell parameter (4.213 Å) and bulk modulus (160 GPa) [23] very well. Calculated enthalpies of MgO as a function of pressure are summarized in Table 5.

In order to evaluate the stability of Al^{3+} incorporation into $MgSiO_3$ perovskite, we have assumed a mineral reaction given by:

$$Mg_{n-1}Al_2Si_{n-1}O_{3n} + 2MgO = Mg_nAl_2Si_{n-2}O_{3n-1} + MgSiO_3 \quad (1)$$

We have chosen $2\times2\times1$ super-cells in which we substituted two Al^{3+} ions, thus $n=16$. Eq. 1 represents the reaction (from left to right) from charge-coupled substitution to oxygen-vacancy substitution. In order to investigate how Al ions are incorporated into $MgSiO_3$ perovskite, we calculated the enthalpy differences, ΔH, for Eq. 1, i.e. $\Delta H = \{H(Mg_{16}Al_2Si_{14}O_{47}) + H(MgSiO_3)\} - \{H(Mg_{15}Al_2Si_{15}O_{48}) + 2H(MgO)\}$, in which enthalpies of CCM1 for all pressures, of OVM4 for zero pressure and of OVM1 for pressures between 25 and 100 GPa are employed. Results for enthalpy changes as a function of pressure are shown in Fig. 3. The enthalpy difference ΔH is positive at all pressures from 0 to 100 GPa as shown in Fig. 3. This means Al ions should be able to go into $MgSiO_3$ perovskite through CCM, which is more favored than OVM at all pressures up to 100 GPa. Recent Al XAFS [15] and NMR [16] experiments suggested that CCM should be the most likely mechanism, and the empirical molecular-mechanics simulations [14] also suggested that the CCM mechanism is more favorable than OVM at lower mantle pressure ranges. In contrast, the recent first-principles DFT results by Brodholt [18] suggested OVM should be favored at shallower parts of the lower mantle up to about 30 GPa, and CCM is favorable at higher pressures. In his calculations, however, he discussed the enthalpy change of a reaction expressed by:

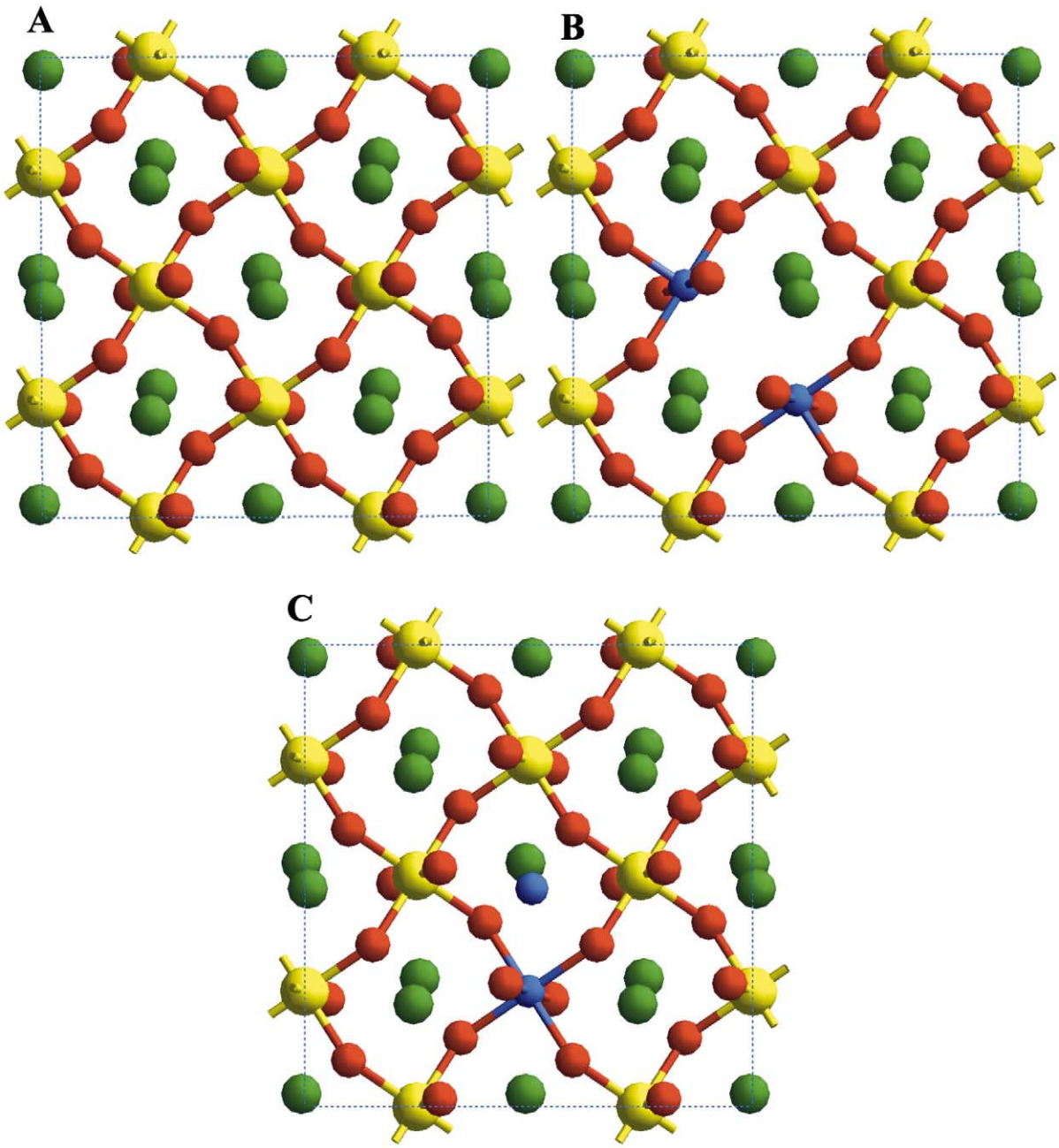

Fig. 2. Projections along the *c* axis of the calculated super-cells optimized at 25 GPa for (A) Al-free and two models of aluminous perovskites, (B) OVM1 and (C) CCM1. Yellow, green, red and blue balls denote Si, Mg, O and Al ions, respectively. Nearest-neighbor pairs of two Si^{4+} ions and of Mg^{2+} and Si^{4+} are replaced by two Al^{3+} ions in these two Al-incorporated models, OVM1 and CCM1, respectively. Note that the oxygen vacancy exists between the two substituted Al^{3+} ions (blue balls) in panel B, whereas no oxygen vacancy exists in panel C.

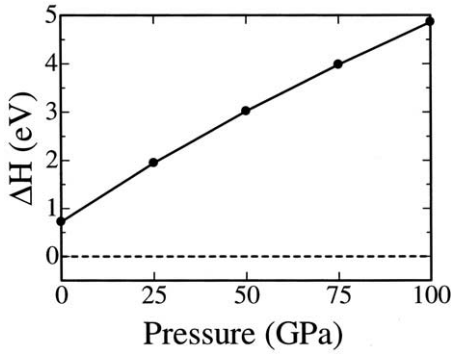

Fig. 3. Calculated enthalpy difference, ΔH, for the reaction in Eq. 1 as a function of pressure.

$$(Mg_3Al)(Si_3Al)O_{12} + 2MgO = Mg_2Al_2O_5 + 3MgSiO_3 \quad (2)$$

in which $(Mg_3Al)(Si_3Al)O_{12}$ perovskite corresponding to 25 mol% Al_2O_3 incorporation was employed for CCM and no Si was taken into account for OVM in the $Mg_2Al_2O_5$ brownmillerite. Moreover, only highly ordered substitution can be manifested with these $(Mg_3Al)(Si_3Al)O_{12}$ perovskites and $Mg_2Al_2O_5$ brownmillerites. In our first-principles DFT calculations, a larger super-cell with 80 atoms was employed and a more realistic concentration, i.e. 6.25 mol% Al_2O_3 incorporation, was examined, and they showed lower-oriented substitutions. Therefore, our calculations yield a different result in that CCM for incorporating Al^{3+} is found to be more favorable than OVM at lower mantle pressures. This finding completely supports the experimental findings [15,16].

Table 5
Calculated enthalpies, H, as a function of pressure, P, for MgO and Al_2O_3

P (GPa)	H(MgO) (eV)	$H(Al_2O_3)$ (eV)
0	−1419.31	−1438.90
25	−1416.46	−1432.86
50	−1413.90	−1427.25
75	−1411.54	−1421.94
100	−1409.32	−1416.89

Enthalpies are transferred to the ones for unit chemical formulae.

To examine the feasibility of the Al^{3+} ion to be substituted into $MgSiO_3$ perovskite via CCM and OVM, we calculated the enthalpy differences for the two reactions expressed by:

$$(n-1)MgSiO_3 + Al_2O_3 = Mg_{n-1}Al_2Si_{n-1}O_{3n} \quad (3)$$

for CCM substitution, and

$$(n-2)MgSiO_3 + 2MgO + Al_2O_3 = Mg_nAl_2Si_{n-2}O_{3n-1} \quad (4)$$

for OVM substitution. Here we choose $2\times2\times1$ cells, which yield $n=16$. The enthalpy difference, ΔH, between left and right hand sides of Eqs. 3 and 4, i.e. $\Delta H = H(Mg_{15}Al_2Si_{15}O_{48}) - \{H(15MgSiO_3)+H(Al_2O_3)\}$ for CCM and $\Delta H = H(Mg_{16}Al_2Si_{14}O_{47}) - \{H(14MgSiO_3)+2H(MgO)+H(Al_2O_3)\}$, are summarized in Table 6. We have used the enthalpy for Al_2O_3 with the corundum structure, which is shown in Table 5 together with the one for MgO. All the enthalpy differences, which correspond to the formation enthalpies of aluminous Mg-perovskite via CCM and OVM, are positive, as shown in Table 6, in which ΔH does not change much in the case of CCM, while it increases in the case of OVM with greater pressure. The calculated enthalpy differences for CCM are smaller than those for OVM at all pressures. This result also shows that Al is more soluble in Mg-perovskite via CCM than OVM.

Table 6
Calculated enthalpy differences, ΔH, between left and right hand sides of Eqs. 3 and 4 for CCM and OVM, respectively

P (GPa)	ΔH (eV)				
	OVM1	OVM2	OVM3	OVM4	OVM5
0	2.07	2.07	2.26	2.01	2.12
25	3.45	3.89	3.89	3.66	4.04
50	4.52	5.13	5.13	4.89	5.47
75	5.40	6.15	6.15	5.92	6.61
100	6.23	7.10	7.10	6.84	7.66
	CCM1	CCM2	CCM3	CCM4	CCM5
0	1.34	1.45	1.45	1.52	1.42
25	1.51	1.53	1.56	1.67	1.58
50	1.51	1.53	1.63	1.71	1.62
75	1.42	1.48	1.53	1.67	1.57
100	1.36	1.39	1.50	1.65	1.56

Our calculations have been performed with the static first-principles method. However, entropy considerations could have a significant effect on relative stabilities of the various models at real mantle temperatures. Although a Monte Carlo or molecular dynamics simulation might be more appropriate to account for configurational contributions to the entropy, the first-principles static calculations at 0 K cannot take the thermal effects into consideration. Although our calculations show that CCM is more favorable than OVM at all pressures, as shown in Fig. 3, the calculated enthalpy difference between these two substitutions at lower pressures is not so large. Hence OVM may coexist with CCM at lower pressures if we take into account the entropic contributions.

4. Conclusions

In this paper we have performed large-scale density functional calculations to investigate in detail the substitution mechanism of Al ions being incorporated into $MgSiO_3$ perovskite and also the change in the compressional mechanism of aluminous perovskite in the lower mantle. To study the substitution mechanism, we considered 10 substitution configurations for OVM and CCM at five pressure points between 0 and 100 GPa, i.e. 50 calculating points are examined in total. These calculations show that the CCM1, in which a nearest pair of Mg^{2+} and Si^{4+} is replaced by two Al^{3+} ions, should be more favorable than any other CCMs and OVMs at pressures up to 100 GPa. This result is consistent with the experimental XAFS [15] and NMR [16] results. The calculated bulk modulus of the most favorable Al-incorporated $MgSiO_3$ perovskite, CCM1, is -3.4% relative to that of Al-free perovskite. Our result shows the same trend as the experiments, although our first-principles calculations are not able to explain fully the reduction of 10% in the bulk modulus [11]. We have raised the interesting question regarding the sensitivity of the elastic parameters to the presence of Al-perovskite in the lower mantle. Recent results by Deschamps and Trampert [24] have found that if Al-perovskite is present only in 3–4% in volume, then the mid-mantle geotherm can be lowered by 150–200 K. Future ab initio calculations incorporating lattice dynamics effects [25] are needed to verify this effect of Al-perovskite on the determination of the mantle geotherm.

Acknowledgements

We thank Prof. Anne Hofmeister and two anonymous reviewers for helpful comments. Drs. T. Iitaka and T. Morishita, RIKEN, are acknowledged for their careful reading and useful comments on the manuscript. Dr. J. Trampert is acknowledged for fruitful discussions and providing us with a preprint. The authors would like to thank the United Kingdom Car-Parrinello (UKCP) consortium for providing us with the academic version of CASTEP. One of the authors (T.Y.) acknowledges the Special Postdoctoral Researchers Program in RIKEN.*[SK]*

References

[1] R. Boehler, High-pressure experiments and the phase diagram of lower mantle and core materials, Rev. Geophys. 38 (2000) 221–245.
[2] B.B. Karki, L. Stixrude, Seismic velocities of major silicate and oxide phases of the lower mantle, J. Geophys. Res. 104 (1999) 13025–13033.
[3] G.R. Helffrich, B.J. Wood, The Earth's mantle, Nature 412 (2001) 501–507.
[4] H. Horiuchi, E. Ito, D.J. Weidner, Perovskite-type $MgSiO_3$: Single-crystal X-ray diffraction study, Am. Mineral. 72 (1987) 357–360.
[5] G. Fiquet, A. Dewaele, D. Andrault, M. Kunz, T. Le Bihan, Thermoelastic properties and crystal structure of $MgSiO_3$ perovskite at lower mantle pressure and temperature conditions, Geophys. Res. Lett. 27 (2000) 21–24.
[6] R.M. Wentzcovitch, J.L. Matins, G.D. Price, Ab initio molecular dynamics with variable cell shape: application to $MgSiO_3$, Phys. Rev. Lett. 70 (1993) 3947–3950.
[7] R.M. Wentzcovitch, B.B. Karki, S. Karato, C.R.S. Da Silva, High pressure elastic anisotropy of $MgSiO_3$ perovskite and geophysical implications, Earth Planet. Sci. Lett. 164 (1998) 371–378.
[8] M. Matsui, G.D. Price, Simulation of the pre-melting behavior of $MgSiO_3$ perovskite at high pressures and temperatures, Nature 351 (1991) 735–737.
[9] B.B. Karki, L. Stixrude, S.J. Clark, M.C. Warren, G.J.

Ackland, J. Crain, Elastic properties of orthorhombic $MgSiO_3$ perovskite at lower mantle pressures, Am. Mineral. 82 (1997) 635–638.
[10] A.R. Organov, J.P. Brodholt, G.D. Price, The elastic constants of $MgSiO_3$ perovskite at pressures and temperatures of the Earth's mantle, Nature 411 (2001) 934–937.
[11] J. Zhang, D.J. Weidner, Thermal equation of state of aluminum-enriched silicate perovskite, Science 284 (1999) 782–784.
[12] A. Kubo, T. Yagi, S. Ono, M. Akaogi, Compressibility of $Mg_{0.9}Al_{0.2}Si_{0.9}O_3$ perovskite, Proc. Jpn. Acad. B76 (2000) 103–107.
[13] T. Irifune, Absence of an aluminous phase in the upper part of the Earth's lower mantle, Nature 370 (1994) 131–133.
[14] N.C. Richmond, J.P. Brodholt, Calculated role of aluminum in the incorporation of ferric iron into magnesium silicate perovskite, Am. Mineral. 83 (1998) 947–951.
[15] D. Andrault, D.R. Neuville, A.M. Flank, Y. Wang, Cation sites in Al-rich $MgSiO_3$ perovskites, Am. Mineral. 83 (1998) 1045–1053.
[16] J.F. Stebbins, S. Kroeker, D. Andrault, The mechanism of solution of aluminum oxide in $MgSiO_3$ perovskite, Geophys. Res. Lett. 28 (2001) 615–618.
[17] M.C. Payne, M.P. Teter, D.C. Allan, T.A. Arias, J.D. Joannopoulos, Iterative minimization techniques for ab initio total-energy calculations: molecular dynamics and conjugate gradients, Rev. Mod. Phys. 64 (1992) 1045–1097.
[18] J.P. Brodholt, Pressure-induced changes in the compression mechanism of aluminous perovskite in the Earth's mantle, Nature 407 (2000) 620–622.
[19] W.A. Harrison, Applied Quantum Mechanics, World-Scientific, 2000, 372 pp.
[20] J.P. Perdew, S. Burke, M. Ernzerhof, Generalized gradient approximation made simple, Phys. Rev. Lett. 77 (1996) 3865–3868.
[21] D. Vanderbilt, Soft self-consistent pseudopotentials in a generalized eigenvalue formalism, Phys. Rev. B41 (1990) 7892–7895.
[22] H.J. Monkhorst, J.D. Pack, Special points for Brillouin-zone integrations, Phys. Rev. B13 (1976) 5188–5192.
[23] Y. Fei, Effects of temperature and composition on the bulk modulus of (Mg, Fe)O, Am. Mineral. 84 (1999) 272–276.
[24] F. Deschamps, J. Trampert, Constraining the lower mantle reference temperature: what is possible?, submitted to Earth Planet. Sci. Lett.
[25] C.R.S. Da Silva, R.M. Wentzcovitch, A. Patel, G.D. Price, S.I. Karato, The composition and geotherm of the lower mantle: constraints from the elasticity of silicate perovskite, Phys. Earth Planet. Inter. 118 (2000) 103–109.